Micro-gravity Isolation using only Electro-magnetic Actuators

Vinther, D.; Alminde, Lars; Bisgaard, Morten; Viscor, T.; Østergaard, Kasper Zinck

Publication date:
2004

Document Version
Publisher's PDF, also known as Version of record

MICRO-GRAVITY ISOLATION USING ONLY ELECTRO-MAGNETIC ACTUATORS

Lars Alminde, Morten Bisgaard, Dennis Vinther, Tor Viscor, and Kasper Østergaard

Department of Control Engineering, Aalborg University, Fredrik Bajers Vej 7C, DK-9220 Aalborg Øst, Denmark, {*lalm00, mbis00,drvi00,tvis00,kzoe00*}*@control.aau.dk*

Abstract: The subject discussed in this paper is the design, construction and test of a free floating micro-gravity isolation platform to reduce the acceleration dose on zero gravity experiments on e.g. the International Space Station (ISS). During the project a system is specified and constructed whereupon it is tested in the sixth student parabolic flight campaign issued by the European Space Agency (ESA). The system consists of six custom made electro magnetic actuators which acts on the isolated platform based on the designed controller and their input from six accelerometers and six infrared position sensors.
From the data acquired during the flights it is concluded that the control algorithm used to position the platform fulfills the requirements, but it is not yet possible to draw final conclusions on the performance of the acceleration controller. It does, however, indicate a better performance, but better sensors are required.

Keywords: Magnetic, Actuators, Automatic Control

1. INTRODUCTION

One of the major features of the space-environment is the lack of gravity that makes it possible to conduct research that is practically impossible on the surface of the Earth. Many fields of science use this environment for experiments, examples include cultivation of non-organic crystals, cultivation of various long proteins, combustion physics, as well as space medicine.

Currently facilities on-board the International Space Station (ISS), the Space Shuttle and dedicated recoverable satellites, such as the Russian Foton, are used to conduct experiments in zero gravity. However, when using these crafts as research laboratories there are a number of factors that influence the environment and changes it from a theoretically zero-gravity environment to a micro-gravity (μg) environment. These factors include:

(1) Spacecraft maneuvering
(2) Gravity forces due to spacecraft mass distribution
(3) Residual atmospheric drag on spacecraft structures
(4) Structural vibrations due to spacecraft and/or crew activity

These disturbances to the μg environment degrades the performance of many types of μg-experiments, and for many types the performance is proportional to the quality of the μg-environment under which the experiment is conducted. As an example it can be said that the residual acceleration level experience on the Space Shuttle is in the vicinity of $10^{-4}g$ (Rogers *et al.*, 2003). Therefore there is a need for systems that can be used to isolate the experiments con-

ducted on the spacecrafts from the structural vibrations either through passive or active compensation. Complete isolation is by all means impossible and the task is then reduced to make the system compensate such that the experiment experiences the smallest possible dose of acceleration.

The most recent and most promising system is called G-limit (see (Whorton, 2003)), which has been developed by NASA over the last 5 years. It uses three dual axis electro-magnetic actuators, and thereby provides stabilization in six degrees of freedom. The G-limit system has not yet been flown, but was scheduled to fly on the Space Shuttle, when the shuttle fleet becomes operational again, following the Columbia disaster.

The goal of the MIEMA project is to develop a system that fundamentally uses the same techniques as the G-limit system in order to provide a stabilized μg environment, i.e. both systems will use electro-magnetic actuators and measurements of platform acceleration and positions in order to stabilize the experiment. The difference between the two projects will be the actual actuator design principles and the control algorithms. The MIEMA project will use six single-axis actuators compared to the three dual-axis on G-limit. This difference as well as the possible control algorithm designs makes it possible to evaluate performance on a system that is similar, but yet different, to the existing G-limit system.

The MIEMA project has had the opportunity to evaluate the design in the sixth student parabolic flight campaign and the results gained there will be presented in this paper. Based on the results from the campaign then ESA has chosen the experiment to re-fly on the 36th ESA Parabolic Flight Campaign in March 2004. Essentially this will be a reflight of the same configuration, but with a number of identified hardware and software issues solved, as well as a general reiteration of the control algorithms based on the flight results.

2. CONCEPTUAL AND MECHANICAL DESIGN

The basic setup for MIEMA is a free-floating Isolated PLatform (IPL) shaped as a disc on which the μg critical experiments can be placed. The idea of making the IPL free-floating is to reduce the disturbance coupling from the environment by removing mechanical contact.

2.1 Performance Requirements

In order to derive the requirements for the MIEMA system a set of initial requirements, focusing on performance, will be proposed using the ISS μg requirements as a reference. The vibrations on the ISS can be divided into three distinct categories (Whorton *et al.*, 2002): Low frequencies (below 10^{-3} Hz), intermediate frequencies (10^{-3} to 1 Hz) and high frequencies (above 1 Hz).

Low frequent originate from atmospheric drag and are non-transient.

Intermediate frequent originate mostly from motion of astronauts, equipment and from motion of ISS when using thrusters. These vibrations are mainly transient.

High frequency exists in two different types; transient from astronaut motion and mechanical impacts, and sinusoidal from pumps, motors etc.

The desired acceleration level on-board ISS as well as the actual measured acceleration is shown on figure 1 (Whorton *et al.*, 2002). The desired levels have been specified by NASA's Principal Investigator for Micro-gravity Services (PIMS) that coordinates all μg research on ISS. From the figure it can be seen that there is a need for attenuation of the accelerations to fulfill the desired levels.

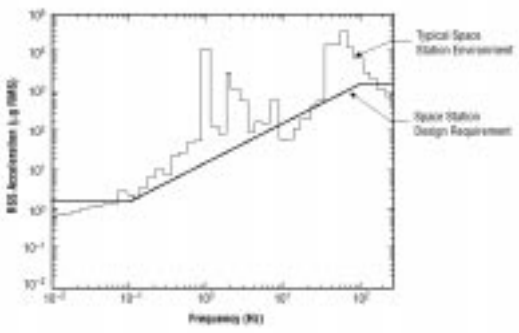

Fig. 1. ISS Micro-gravity requirements and typical actual accelerations.

The actual required attenuation to bring the acceleration level down to an acceptable level have been specified by the PIMS (Whorton, 2002) which are shown on figure 2

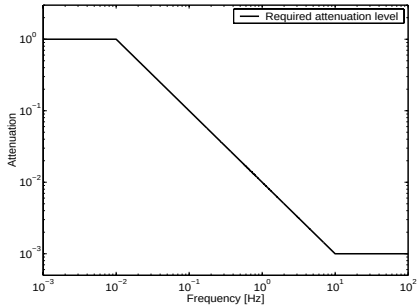

Fig. 2. The required attenuation level.

However, due to the financial limitations of this student project it turned out that it was im-

possible to acquire acceleration-sensors capable of fulfilling NASA's requirements of 1 μg and as the project is a demonstration-project is was chosen to scale the requirements with a factor of 200 yielding a lower limit of 200 μg as this fits the quality of sensors it was possible to acquire. This however creates very large displacements at low frequencies and a limit of $\pm$5 mm displacement was set which creates a lower limit for disturbance-attenuation of 0.1 Hz instead of 0.01 Hz in the original requirements which again moves the scale in figure 2 up by one decade.

2.2 Actuators and Sensors

Disturbances originating from crew activity, mechanical vibrations and space-craft movements can be introduced in the isolated system in two different ways: As translational (linear) motion and as rotational motion. This implies that the system can be disturbed along six degrees of freedom (DOF) and the system must therefore be able to actuate the IPL in six DOF as well. In order to accommodate this it was chosen to utilize six electro-magnetic actuators mounted with three on the sides and three under the IPL as shown in figure 3.

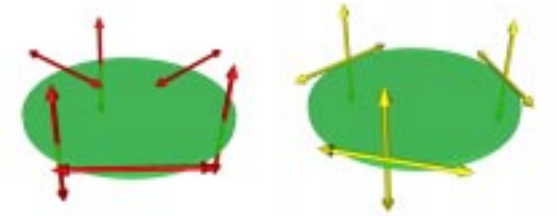

Fig. 3. Left: illustration of actuator forces on the IPL which also collides with the placement of the position sensors. Right: placement of the acceleration sensors.

Two different sensor systems are used for the control of the IPL: Position and acceleration sensors. Both sensor systems are positioned on the system in such a way that they cover all six DOF as with the actuators.

The position sensor are used to keep track to displacements of the IPL which originates from very low frequency disturbances and for this simple IR-sensors have been designed which features a precision of 0.5 mm using measurements of reflected light-intensity. The acceleration sensors make up the primary sensor system of MIEMA and are used to measure the accelerations and thereby the g-level of the IPL. These measurements can then be used in a control-loop to attenuate the vibration of the IPL. The needed resolution and bandwidth for the sensor must be at least 200 μg and 100 Hz which the ASA7002 from Honeywell

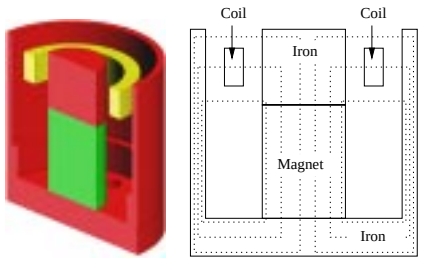

Fig. 4. Left: 3D actuator configuration. Right: cross section of magnetic field of the actuator.

satisfy with a fair compromise of performance and prize.

2.3 Actuator design

The choice of electro-magnetic actuators came from the option of constructing non-contact actuators thereby reducing the disturbances imposed on the IPL. The design adopt principles from speaker-designs as the actuators are created as voice-coils as this principle gives the possibility (and advantage) of creating linear actuators and consists of a permanent magnet part that create a magnetic field, and a current-conducting coil by which the force of the actuator can be created. Magnetic fields are normally considered highly non-linear, but by using a principle as shown in figure 4 with a permanent magnet and iron, used to channel the magnetic field, it is possible to create a strong and relatively uniform field in the working area of the coil and a weak magnetic field outside the actuator.

The requirements for the actuators are that they must have a bandwidth wide enough to cover the frequencies up to at least 100 Hz while still being able to operate at very low frequencies. Also they must allow a stroke of at least the maximum displacement of 5 mm in all directions as shown in the last subsection. This displacement requirement is both valid for the direction of the actuation of the particular actuator, as well as the direction perpendicular to the actuation direction.

2.4 Mechanical Design

The entire IPL has been constructed in aluminum, the reason for this is that aluminum has a very high magnetic resistance, and magnetic fields traveling through the system is therefore of no concern. In figure 5 the fully mounted IPL is shown, and the three side actuator-coils can be seen, as well as signal processing hardware on top of the disc.

The permanent part of the actuators were mounted onto a base-plate and a lexan-glass box was constructed around it, which should contain the IPL

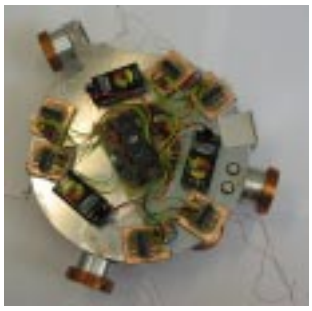

Fig. 5. IPL with coils, sensors and electronics.

in case of a crash during the zero-g flight campaign. In figure 6 the entire setup is shown with the PC used for the controller shown as the solid box.

Fig. 6. The entire experiment setup.

3. MODELING AND CONTROL

This section describes the modeling and controller design for MIEMA.

3.1 Modeling

The model consists of a dynamic model of the actuators, a static model of the IPL and of transformations between the placement of the actuators and sensors as well as the coordinate-system of the IPL and the outside structure (IST). In figure 7 the complete model is shown where it can be seen that the actuators deliver a force to the IPL (modeled by its mass m) which generates the controlling accelerations (a_{act}) and introduces a back-emf term back into the actuators.

The actuator accelerations are then transformed into the IPL coordinate system. The disturbance accelerations comes from the IST which is transfered to the IPL by a coupling w. The actual movements of the IPL is found as the difference between the accelerations of the IPL and the IST (denoted diff by subscript) which is integrated twice in order to yield the displacement that the the position sensors measures. For both sensor systems transformations are inserted in order to

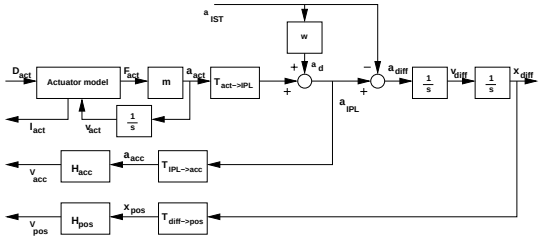

Fig. 7. The complete model of system.

show the system movements at the positions of the sensor.

The transformations between the IPL and both the actuators and the acceleration sensor are non-singular matrices that describe rotations and projections of the accelerations. However, the transformation related to the position sensor is highly non-linear and has been implemented as a seven step recursive algorithm.

3.2 Control

The control of the system has two overall well defined purposes: To attenuate disturbances at frequencies above 0.1 Hz and to track disturbances below 0.1 Hz in order to minimize displacements at low frequencies. The control scheme features three cascaded controllers as shown in figure 8.

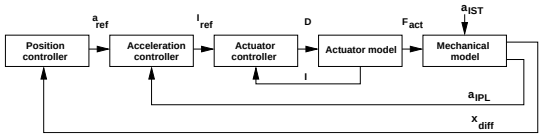

Fig. 8. The overall control scheme for the system.

The inner loop consist of an analog implemented lag controller which reduces the influence of back-emf and other disturbances in the actuators as well as increases the bandwidth of the actuators as seen from the outer loops.

The middle loop is the acceleration loop which is the main control loop that must attenuate disturbances while still being able to track references from the outermost loop. The controller is designed through transform technique design methods and it displays low-pass filter characteristics with a third order pole placed around 100 Hz. Through the design a lot of focus has gone into avoiding resonances as it is very undesirable that the controller actually amplifies disturbances at certain frequencies.

The outer loop is the position loop which is created through a state space design with a reduced order observer. This design enables the controller to move the two poles on the imaginary-axis into the left-half plane and thereby create a low-pass filter with a break frequency around 0.1 Hz.

4. RESULTS FROM FIRST TEST CAMPAIGN

This section will describe the results that was gained from the student parabolic flight campaign during the summer of 2003. Focus will be on the performance of the implemented position controller, and the controllers effect on the microgravity environment. However, in comparison to the baseline design described above then the configuration flown was not fully implemented at the time. The differences were:

- Accelerometers with less sensivity were used, due to unresolved hardware issues at the time
- No active acceleration control was performed, due to the latter point

During the data analysis phase it was discovered that one of the acceleration sensors had malfunctioned. Therefore the following analysis is based only on the Z-axis when discussing acceleration, as this axis was completely unaffected by the malfunction.

4.1 Effectiveness of Implemented Controller

Figure 9 shows the typical result in terms of translational and rotational position respectively from one of the 31 parabolas on the second flight (VOL 188). From the figure it can be observed that the zero-g phase starts at T=4s, then it takes about 5 seconds for the controllers to position the isolated platform near the center, and then follows roughly 7 seconds with good performance, hereafter, at t=16s, control again becomes difficult when the A300 starts to leave the zero-g phase.

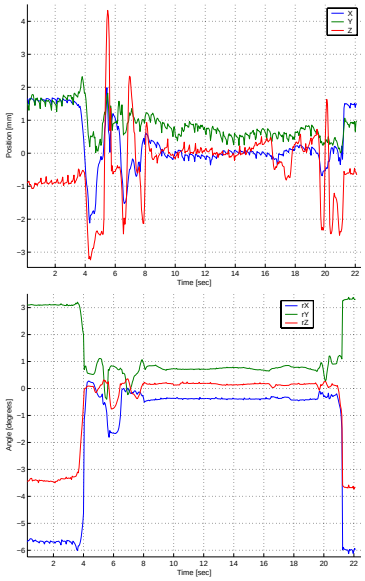

Fig. 9. Translational (TOP) and rotational (BOTTOM) positions during a representative parabola.

It should be noted that the output of the position sensors are not valid during the high-g phases. For all translational sensors the freedom is +/-5mm and for the rotational +/-6 degrees.

In the injection phase the controllers must counter two phenomenas; firstly due to the just due -2 g phase the integral state is presently in positive saturation, and secondly at the start of the zero-g phase a slight positive g is experienced. Combined these effects make the controller overshoot the target considerably before the integral-state is brought out of saturation and close to zero contribution.

This overshoot then results in a slow oscillation, while the experienced acceleration in the A300 slowly declines to near zero. At this point the oscillations have decayed almost to zero.

During the part of the zero-g phase where the acceleration are stable and near zero the controllers are able to keep all translational and rotational positions fairly close to 0.

The reason why the Y-rotation is maintained slightly positive can be explained from the fact that it suffers from the worst disturbance during this part of the zero-g phase, due to the fact that the A300 rotates about its own Y-axis (pitch) from a nose-up elevation at 47 degrees to a nose down elevation of 45 degrees. However, due to the malfunction of the acceleration sensor this disturbance cannot be analyzed in more detail than allowed by the position measurements.

Close to "pull-out" the experienced acceleration in the Z-axis begins to fluctuate before it drops rapidly, as can be seen on the typical graph of figure 9. This phenomena can also be seen on the position graphs, where it can be seen that the position begins to fluctuate, but in general is kept within the admissible range for free-floating operation of the isolated platform until around t=19, where more violent fluctuations begin as the A300 pulls out.

4.2 Improvement in the Zero-g Environment

The effect of the successful position control should be visible in the recorded acceleration data as the platform successfully is mechanically decoupled from the A300. To measure the effect on the μg-environment two plots are presented: figure 10 TOP shows an FFT of the recorded acceleration during the zero-g phases over a series of 30 parabolas with position control, and figure 10 BOTTOM show an FFT of the recorded acceleration during the zero-g phases over a series of 30 parabolas where the isolated platform was kept mechanically coupled to the external platform using the electro magnets.

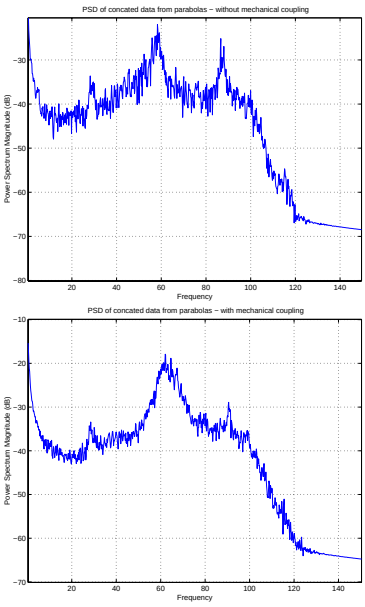

Fig. 10. FFT of recorded Z-axis data. TOP: Controlled parabolas. BOTTOM: With mechanical coupling.

Directly comparing the two graphs yields ambiguous results as they both have regions with better performance. It should be noted that the high acceleration level near DC is due to biases in the measurement circuitry and therefore not relevant for the analysis. If the average value of the power-spectrum is calculated in the frequency range from 1Hz to 100Hz then figure 10 BOTTOM gives a level of $5.08 \cdot 10^{-4}g$, while figure 10 TOP yields $1.67 \cdot 10^{-4}g$. This corresponds to a general reduction of vibration levels of 10dB within the frequency-band of interest.

However, this figure is associated with a lot of noise and can only be considered as an indication that the implemented control system is a step in the correct direction. The inherent problem seems to be that the noise of the implemented sensors are in fact close to the noise level of the A300 environment during zero-g phases, and it is thus difficult to conclude any performance increase with certainty. The next flight therefore calls for better accelerations sensors in order to be able to measure the performance gain in the μg-environment.

4.3 Conclusion on Results

In summary the results show that the designed control algorithms fulfill the requirement regarding positioning of the isolated platform as it is brought close to the reference position during the zero-g phase and kept there while the disturbances are reasonable, i.e. before pull-out.

From the presented plots it was found that the 2g phase presents a problem for the integral states of the controllers, and this is therefore subject for improvement. From the acceleration data it has been concluded that while the data indicates better performance, more sensitive sensors on the next flight opportunity is required to prove this with certainty.

5. CONCLUSION

In conclusion it can be said that so far the MIEMA experiment has been a success. Within the course of 5 months the system was specified, designed, built and tested on the Sixth Student Parabolic Flight Campaign. Technically the tests demonstrated that all the design decisions taken were reasonable and the system worked as intended. As for performance many things can be altered on the current system to improve it. In general obtainable performance is mainly a question of available funding in order to buy precision sensor components.

As a second flight opportunity has been granted then this opportunity will be used to test basically the same system, but with the following additions and improvements:

- Functional precision accelerometers (baseline sensors)
- Included explicit acceleration control
- Reiterated algorithms based on previous flight results
- A set of precision accelerometers placed on IST for better comparison between the fixed and floating part of the system

This opportunity will be used to reconfirm the findings reported here with higher sensivity on acceleration data by a factor of 60, and the improvements, namely the inclusion of active acceleration control, should also make it possible to achieve better performance than what has been reported here.

REFERENCES

Rogers, Melissa J. B., Gregory L. Vogt and Michael J. Wargo (2003). *Microgravity a Teacher's Guide with Activities in Science, Mathematics and Technology*. NASA.

Whorton, Mark (2002). *Fundamentals of Microgravity Vibration Isolation*. NASA.

Whorton, Mark (2003). *G-limit homepage*. NASA. spacere-search.nasa.gov/research_projects/ros/glimit.html.

Whorton, M.S, J.T. Eldrige, R.C. Ferebee, J.O. Lassiter and J.W. Redmon (2002). *Damping Mechanisms for Microgravity Vibration Isolation*. NASA.